The Catalytic Role of the W573 in the Mobile Loop of Recombinant Acetohydroxyacid Synthase from Tobacco

Masud Karim, Mi-Young Shim, Joungmok Kim, Kyoung-Jae Choi, Jung-Rim Kim,[†] Jung-Do Choi,[‡] and Moon-Young Yoon[*]

Department of Chemistry, College of Natural Sciences, Hanyang University, Seoul 133-791, Korea
[*]E-mail: myyoon@hanyang.ac.kr
[†]Department of Applied Chemistry, Hanyang University, Ansan 429-791, Korea
[‡]School of Life Sciences, Chungbuk National University, Cheongju 361-763, Korea
Received January 17, 2006

Acetohydroxyacid synthase (AHAS, EC 2.2.1.6 also referred to as acetolactate synthase) catalyzes the first common step in the metabolic pathway leading to biosynthesis of the branched-chain amino acids in plants and microorganisms. Due to its presence in plants, AHAS is a target for the herbicides (sulfonylurea and imidazolinone), which act as potent inhibitors of the enzyme. Recently, we have shown [J. Kim, D.G. Baek, Y.T. Kim, J.D. Choi, M.Y. Yoon, *Biochem. J.* (2004) 384, 59-68] that the residues in the "mobile loop" 567-582 on the C-termini are involved in the binding/stabilization of the active dimer and ThDP (thiamin diphosphate) binding. In this study, we have demonstrated the role of the W573 in the mobile loop of the C-termini of tobacco AHAS. The substitution of this W573 residue caused significant perturbations in the activation process and in the binding site of ThDP. Position W573 plays a structurally important role in the binding of FAD, maintaining the enzyme active site in the required geometry for catalysis to occur. In here we propose that the tryptophan at position 573 is important for the catalytic process.

Key Words : Acetohydroxyacid synthase, Kinetics, Fluorescence, Site-directed mutagenesis

Introduction

AHAS catalyzes the condensation of two molecules of pyruvate to form acetolactate in the biosynthesis of valine and leucine, or the condensation of pyruvate and 2-keto-butyrate to form 2-aceto-2-hydroxybutyrate in the bio-synthesis of isoleucine.[1,2] AHAS uses thiamine diphosphate (ThDP) as a cofactor in the condensation reactions, and also requires a divalent metal ion that anchors ThDP in the active site as it is for other ThDP-dependent enzymes. AHAS has an essential requirement for FAD, which is unexpected because the reaction involves no oxidation or reduction. The first two cofactors are typical for enzymes that catalyze the decarboxylation of 2-ketoacids, as occurs in the first stage of the AHAS reaction. The requirement for FAD is not unprecedented and has also been described for glyoxylate carboligase,[3] which is structurally related to AHAS, as well as the unrelated enzyme chorismate synthase.[4]

The crystal structure of the catalytic subunit and AHAS enzyme from yeast was reported at 2.6 Å resolution.[5,6] This structure revealed the location of several active site features, including the position and the conformation of the cofactors ThDP, Mg^{2+} and FAD. The structure, in combination with molecular modeling, also suggested the geometry and location of the binding site for the imidazolinone herbicide imazapyr (2-(4-isopropyl-4-methyl-5-oxo-2-imidazolin-2-yl)nicotinic acid), and provides for a substrates access channel at the interface of the two monomeric subunits. Each monomer has three domains (α, β, and γ). AHAS has two active sites that are on opposite faces of the molecule.

Data from pH studies was consistent with a mechanism in which the ThDP is ionized to the reactive ylide.[7] The resulting carbanion attacks a pyruvate molecule stabilized by delocalization of electrons into the carboxyl probably with the assistance of enzyme residues in the vicinity of the carboxyl. This yields the lactyl-ThDP intermediate via the transiently formed alcoholate anion. After decarboxylation, the enamine of hydroxyethyl-ThDP undergoes charge separation giving the α-carbanion that can now react with a second pyruvate to give the product complex. Finally, the product is released and ThDP is regenerated.

Previously, we studied five mutants (W266F, W439F, W490F, W503F and W573F) of the AHAS gene from *Nicotiana tabacum.*[8] The W490F mutation abolished the binding affinity for cofactor FAD and inactivated the enzyme. The replacement of Trp573 by Phe yielded a mutant AHAS resistant to the three classes of herbicides. The other three mutations, W266F, W439F and W503F, did not affect the enzymatic properties or sensitivity to the herbicides. The structural studies based on the X-ray crystal coordinate (1N0H) of yeast AHAS,[6] have shown that two tryptophan residues (W503' and W586' of yeast AHAS) are observed within 5 Å of ThDP (Fig. 1). Given that W586' is not visible in crystallography of free enzyme without the inhibitor, W503' (corresponding to tobacco AHAS W490) can be postulated to be involved in fluorescence quenching with ThDP. The W573F mutant of AHAS (W586 of yeast AHAS) also showed intrinsic fluorescence quenching with ThDP.[9] Three amino acids that are responsible for herbicide-resistance, Met569, Trp573, and Phe577 have been known
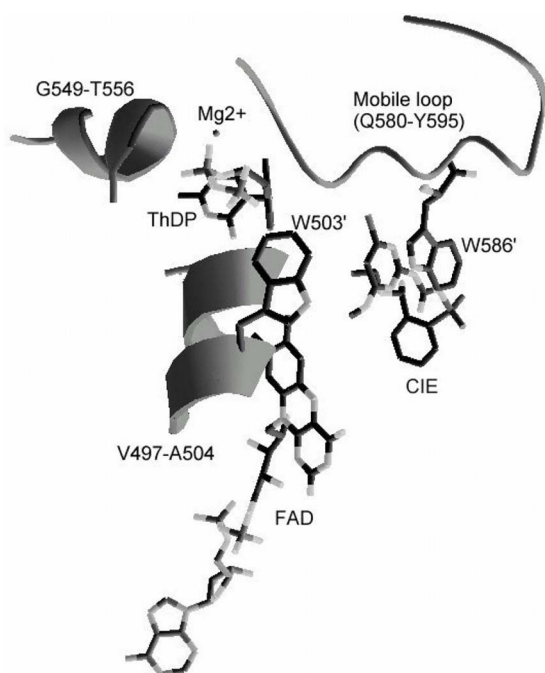
in the putative "mobile loop" region of tobacco AHAS.[9]

To investigate the function of W573 on the γ-domain as a part of the putative "mobile loop" role and the activation process of substrate and cofactors (ThDP, Mg^{2+} and FAD) binding in the active site, we have carried out kinetics, pH studies, thermostability and fluorescence studies of W573F.
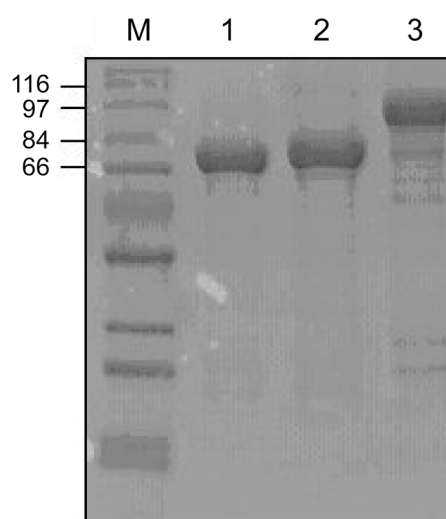
Materials and Methods

Chemicals. Pyruvic acid sodium salt, 4-morpholinepropanesulfonic acid (MOPS), tris(hydroxymethyl)aminomethane, flavin adenine dinucleotide (FAD), thiamin diphosphate (ThDP), α-naphtol, creatine, glutathione, isopropy-β-D-thiogalactoside (IPTG), NaCl, Triton X-100, and $MgCl_2$ were all purchased from Sigma Chemical Co. (St. Louis, USA). Glutathion Sepharose was obtained from Pharmacia Biotech (Uppsala, Sweden). The expression vector pGEX-2T was obtained from Prof. Sang-Ki Paik (Chungnam National University, Taejon, Korea). All other chemicals were obtained from commercial sources and were of the highest quality available.

Expression and purification of enzymes. Expression and purification of the recombinant acetohydroxyacid synthase was performed with modification as described by Chang *et al.*[10] Briefly, *E. coli* DH5α cells containing the expression

Figure 2. SDS-PAGE analysis of purified enzymes. Purified proteins were resolved on a 12% SDS-PAGE gel. The first lane contains molecular weight marker (M), while remaining lanes include purified proteins. These enzymes were overexpressed as N-terminal GST-fusion proteins and purified by the affinity resin, GSH-Sepharose. In addition, GST-free AHASs were generated by the treatment of thrombin described in "Materials and Method" and analyzed on the same SDS-PAGE gel in lane 1, 2 (wild-type AHAS and AHAS W573F, 66 kDa), and lane 3 (N-terminal GST-fusion wild-type AHAS, 94 kDa).

Figure 1. Structure of yeast AHAS active sites showing the relative location of three cofactors (ThDP, FAD, and Mg^{2+}), herbicide, and two tryptophan residues. The active site containing three cofactors was modeled by a SwissProt database program (Deep view) using X-ray coordinates of yeast AHAS (PDB1N0H). The mobile loop region (580-595) was only ordered near the active site in crystal structures of AHAS plus herbicides, chlorimuron ethyl (CIE). Two tryptophan residues, W503' and W586', were corresponded to the residues, W490 and W573 of tobacco AHAS. Partial ribbon diagrams were one part of monomer B of yeast AHAS close to ThDP within 5 Å.

plasmid pGEX-AHAS were grown at 37 °C in Luria-Bertani (LB) medium containing 50 μg/mL ampicillin to an OD_{600} of 0.7-0.8. Cells were induced by the addition 1 mM IPTG and grown for an additional 4 hours at 30 °C. Cells were harvested by centrifugation at 4000 × g for 15 min. The cell pellet for the purification was resuspended in PBST buffer (50 mM sodium phosphate, pH 7.5, 0.15 M NaCl, 1% (v/v) Triton X-100) containing protease inhibitors (2 μg/mL Leupeptin, 4 μg/mL Aprotinin, and 2 μg/mL Pepstatin A). The cell suspension was lysed by sonication at 4 °C. The homogenate was centrifuged at 10,000 × g for 20 min and the supernatant was applied to a GSH-coupled Sepharose column with PBST buffer. The GST-AHAS fusion protein was recovered from the column with an elution buffer (50 mM Tris-HCl, pH 8.0, 20 mM GSH, and 10% (v/v) ethylene glycol). The fusion protein was desalted using desalting column and digested with thrombin protease (2 U/mg protein) for 2 hours at 16 °C. The intact AHAS was purified by another GSH affinity chromatography step (Fig. 2). When FAD-free AHAS was required for particular experiments, FAD was removed from the preparation by adsorption using activated charcoal. The proteins were incubated with 5% (w/v) activated charcoal and 1.6 M KCl in 50 mM Tris-HCl, pH 8.0, for 30 min on ice, and the charcoal was removed by centrifugation. The isolated protein was identified by SDS-PAGE analysis and the protein concentration was determined by the method of Bradford.

Site-directed mutagenesis. Site-directed mutagenesis of tobacco AHAS was performed on the plasmid pGEX-AHAS, using the PCR megaprimer method. The first poly-

merase chain reaction (PCR) was carried out with the universal primer NKB2 and mutagenic primer as internal primer: NKB2, 5'-CCC GGG GAT CCT CAA AGT CAA TAG G-3'; internal primer, 5'-GGT GGT TCA ATT CGA GGA TC-3'. The resulting DNA was subjected to the second PCR with the universal primer NKB1, 5'-CAT CTC CGG ATC CAT GTC CAC TAC CCA A-3'. All DNA manipulations were carried out using techniques reported previously.[8,11,12]

Enzyme assay. Enzyme activities of the wild and mutant AHAS were measured according to the method of Westerfeld[13] with a modification as reported previously.[9,14] The standard reaction mixture contained 100 mM potassium phosphate buffer (pH 7.5), 1 mM ThDP, 10 mM $MgCl_2$, 20 μM FAD, 75 mM pyruvate, and the enzyme. Assays were initiated by the addition of AHAS at 37 °C for 30 min and terminated by the addition of 6 N H_2SO_4. The reaction product acetohydroxyacid was allowed to decarboxylate at 60 °C for 15 min. The acetoin formed by acidification was incubated and colorized with 0.5% creatine and 5% α-naphthol at 60 °C for 15 min. All reactions were carried out in a 1-mL cuvette with a 1 cm-light path-length. UV/vis absorbance spectra were recorded on a Cary 3E UV/vis spectrophotometer. The absorbance of the reaction mixture was monitored at 525 nm. The concentration of reactants was corrected for the concentration of the metal chelate complexes according to Dawson *et al.*[15] One unit (U) of activity was defined as the amount required forming 1 μmol of acetohydroxyacid per minute under the assay conditions described above. Specific activities of AHAS were expressed as units (U) per mg of protein.

Thermostability. Enzymes were preincubated in the buffer containing 100 mM MOPS, pH 7.5, 1 mM ThDP, 20

μM FAD, and 10 mM $MgCl_2$ at the indicated temperatures for 5 min (Fig. 3), and reaction was initiated by the addition of 100 mM pyruvate. Relative activity was determined by the activity at the optimum temperature (37 °C) as a control (100 %).

Quenching of intrinsic protein fluorescence. The substrate or the cofactors-dependent quenching of intrinsic protein fluorescence was monitored as a function of the substrate or the cofactors and the reduction in equilibrium fluorescence was monitored. Duplicate reactions were performed over the indicated concentration range in the presence of AHAS at 25 °C in an initial volume of 500 μL of 100 mM HEPES, pH 7.5 and in the presence and absence of the other cofactors. Samples were excited at 295 nm (4-nm band pass) and were emission at 340 nm (4-nm band pass) in a SLM-Aminco 8100. The final concentration of AHAS used in the experiments was 4 μM. The quenching data was fitted to the following equation by using the program Enzfitter (a non-linear curve fitting program, BIOSOFT):

$$(\Delta F/F_o \times 100) = [(\Delta F_{max}/F_o \times 100)[Q]]/(K_d + [Q]) \qquad (1)$$

Where $\Delta F/F_o \times 100$ is the percent quenching (percent change in fluorescence relative to the initial value) following addition of the quencher at a concentration [Q] and K_d is the dissociation constant.

Kinetic data collection. Reciprocal values of the steady state rate were plotted as a function of the reciprocal of the substrate concentrations. Data was analyzed according to the appropriate rate equations by using the FORTRAN programs of Cleland.[16] Individual saturation curves were fitted to Eq. (2).

$$v = VA/(K + A) \qquad (2)$$

In Eq. (2), A is the reactant concentration. V is the maximum velocity, and K is the Michaelis constant for the varied substrate.

Results

Steady-state kinetic parameter. Substrate saturation curves for the wild-type and W573F AHAS deviated somewhat from a hyperbolic curve as reported previously for wild-type AHAS.[7,17] After removal of the cofactors, wild-type and W573F AHAS showed little or no activity upon adding back any two of them (ThDP, Mg^{2+}, and FAD). Full activity was restored by the addition of the third cofactor with a hyperbolic dependence of the rate upon the cofactor concentration (data not shown). These data were analyzed to determine cofactor activation constants and were fitted to the Hill equation $v_o/E_o = (k_{cat}S^n)/[(S_{0.5})^n + S^n]$, and the parameters were determined from a non-linear least-squares fit. The effect of pyruvate concentration on the rate of reaction was that the saturation curve of W573F did not follow simple Michaelis-Menten kinetics. Although the departure from a hyperbolic curve is rather subtle and might have been disregarded in a single experiment, it was observed consistently in a number of experiments.
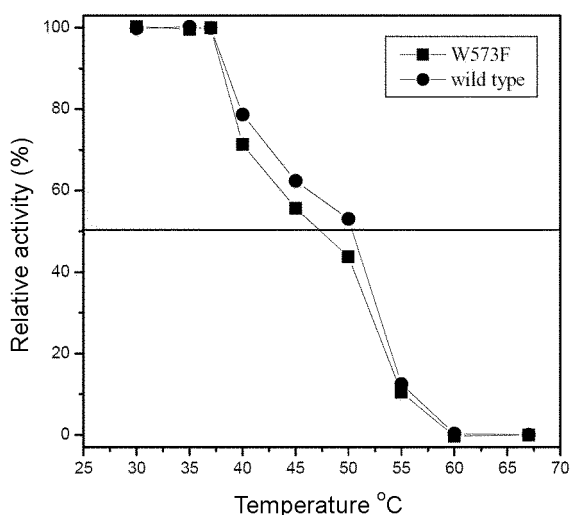
Figure 3. Thermostabilities of wild-type (●) and W573F mutant (■). Enzymes were preincubated in the buffer containing 100 mM MOPS, pH 7.5, 1 mM ThDP, 20 μM FAD, and 10 mM $MgCl_2$ at the indicated temperatures for 5 min, and reaction was initiated by the addition of 100 mM pyruvate. Relative activity was determined by the activity at the optimum temperature (37 °C) as a control (100%).

Table 1. Comparison of the steady-state kinetic parameters of wild-type (WT) and W573F AHAS

	k_{cat} (S^{-1})	K_m (mM)	k_{cat}/K_m ($mM^{-1}S^{-1}$)	n
WT	16.1 ± 0.83	6.53 ± 0.88	2.47	0.75
W573F	5.4 ± 0.87	148 ± 39	0.036	0.86

Table 2. Comparison of parameters of cofactor of wild-type (WT) and W573F AHAS

|	ThDP (mM)	FAD (μM)	$MgCl_2$ (mM)
WT ($S_{0.5}$)	0.78 ± 0.08	1.29 ± 0.30	0.56 ± 0.20
W573F ($S_{0.5}$)	0.23 ± 0.01	4.93 ± 0.39	2.18 ± 0.26
n (WT / W573F)	0.73 / 1.34	0.82 / 1.35	0.70 / 1.01

Table 1 shows the kinetic data of K_m and k_{cat}/K_m for wild-type and W573F obtained by fitting data to Eq. (2) by nonlinear least-squares. The K_m value for W573F was approximately 22-fold higher than that of wild-type, indicating that the substrate binding site is substantially perturbed by the W573F substitution. The k_{cat}/K_m for W573F was approximately 69-fold lower than wild-type AHAS, indicating that W573 seriously affects the catalytic efficiency of the enzyme reaction. The Hill coefficient (n) of W573F (0.86) was similar to that of the wild-type (0.75).

The derived steady-state kinetic parameters of cofactors at pH 7.5 are represented in Table 2. At this pH, the $S_{0.5}$ for wild-type AHAS decreased in the following order: ThDP $\approx$ Mg^{2+} > FAD. However, the $S_{0.5}$ for W573F AHAS decreased Mg^{2+} > ThDP > FAD. The $S_{0.5}$ of Mg^{2+} and FAD in the W573F variant increased approximately 4-fold over wild-type AHAS, but the $S_{0.5}$ of ThDP in the W573 variant decreased approximately 3-fold from that of wild-type AHAS. The Hill coefficients of W573F showed positive cooperativity (1.01-1.35), while that of wild-type showed negative cooperativity (0.70-0.82).

The pH dependence of steady-state kinetic parameters was determined for the wild-type and W573F enzymes. The shapes of k_{cat} versus pH for wild-type and W573F were pH independent (data not shown, also see the reference 17). The Hill coefficients for wild-type and W573F AHAS exhibited were both pH independent.

To test the effect of this substitution at position 573 on the tertiary structure, the thermostability of wild-type and the W573F mutant was examined under the same experimental conditions indicated in Figure 3. The thermostability of the W573F mutant was reduced in relation to that of the wild-type. The T_m for wild-type AHAS was 51 °C, while the T_m value for W573F was reduced by 47 °C.

Intrinsic fluorescence measurements. The intrinsic fluorescence emission spectra for the ThDP of the W573F enzyme are shown in Figure 4. The W573F has a fluorescence emission maximum at 327 nm upon excitation at 295 nm. The data is described by Eq. (1), as shown by the lines in Figure 5; the values of the dissociation constants in Table 3. Titration with pyruvate resulted in a 75% reduction of the initial Trp fluorescence. The dissociation constant (K_d) of
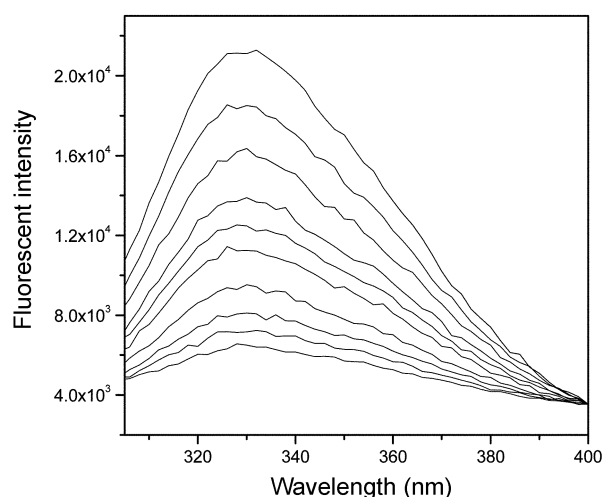

Figure 4. Fluorescence emission spectra of the ThDP saturation in the mutant (W573F) AHAS enzyme. The fluorescence spectra were recorded at 25 °C in 100 mM MOPS buffer, pH 7.5. The emission curves are shown for the ThDP concentration range of 0.0, 0.085, 0.132, 0.168, 0.203, 0.273, 0.339, 0.404, 0.574, 0.741 mM.

pyruvate for the wild-type was 12.31 ± 0.85 mM in the absence of cofactors, and 14.02 ± 0.98 mM for the W573F mutant. The dissociation constant (K_d) of pyruvate for the wild-type was 16.13 ± 1.28 mM in the presence of cofactors (ThDP and Mg^{2+}), and 16.01 ± 0.89 mM for the W573F mutant. These results imply that pyruvate binding in the active site was not affected by the substitution at position 573.

The K_d of ThDP for the wild-type was 0.09 ± 0.002 mM in the absence of cofactors, and 0.11 ± 0.003 mM for the W573F mutant. The affinity (0.34 mM) for ThDP in the presence of any cofactor was similar (0.4 mM) to that of W573F. The K_d of Mg^{2+} for the wild-type was 0.08 ± 0.01 mM in the absence of cofactors, and 0.09 ± 0.01 mM for the W573F mutant. The K_d of Mg^{2+} remained relatively unchanged by the substitution at position 573. The K_d of Mg^{2+} for the wild-type was 0.13 ± 0.01 mM in the presence of ThDP, and 0.15 ± 0.01 mM for the W573F mutant. The K_d of FAD for the wild-type was 23 ± 3.1 μM in the absence of cofactors, and 42 ± 4.8 μM for the W573F mutant. The K_d of FAD for the wild-type was 20 ± 3 μM in the presence of cofactors (0.3 mM ThDP and 1 mM Mg^{2+}), and 40 ± 5 μM for the W573F mutant in the presence of cofactors (0.3 mM ThDP and 1 mM Mg^{2+}).

Discussion

The crystal structures of AHAS enzymes are consistent with a tryptophan residue in the mobile loop (567-582 in tobacco) being conserved.[6] It is therefore surprising that Chong *et al.* were able to mutate this residue in tobacco AHAS to phenylalanine and retain approximately 30% activity.[8] Although this may give rise to some suspicion that this tryptophan is not essential for catalysis, it should be noted that this is an essential hydrophobic residue for
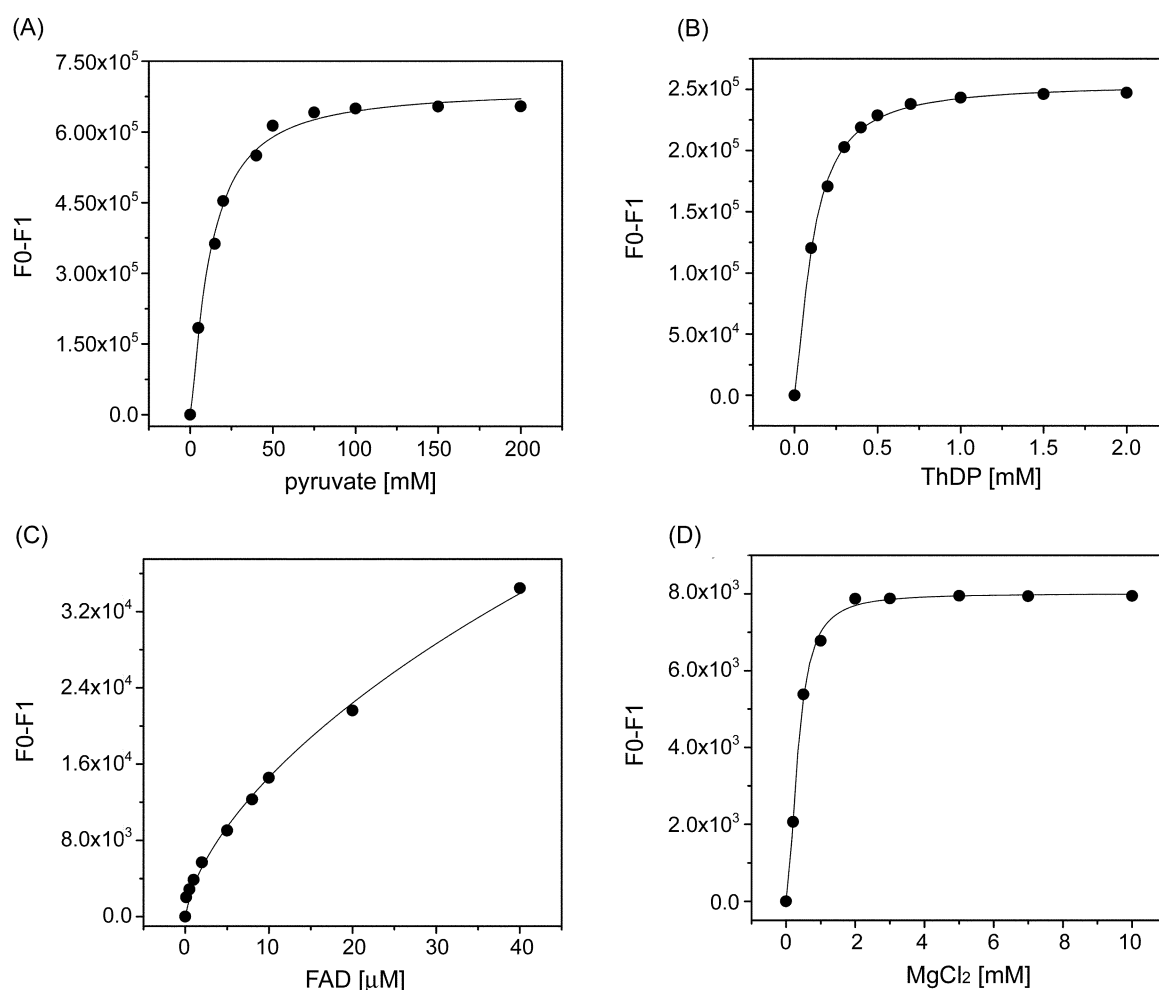
Figure 5. Substrate and cofactor saturation plots for pyruvate (A), ThDP (B), FAD (C), and Mg^{2+} (D) with cofactor (or substrate) concentration shown on a molar scale. Experiments were carried out in 100 mM MOPS buffer, pH 7.5. The curves shown represent the fit of the data to the Hill equation.

Table 3. Parameters of the intrinsic fluorescence quenching of AHAS upon addition of cofactors

		Kd (mM)	Maximal quenching (%)	n
pyruvate	wild-type	16.13 ± 1.28	75.88	1.42
	W753F	16.01 ± 0.89	73.24	1.41
ThDP	wild-type	0.34 ± 0.01	73.79	1.38
	W573F	0.40 ± 0.01	71.10	1.11
FAD	wild-type	0.02 ± 0.003	6.52	1.14
	W573F	0.04 ± 0.005	4.74	1.51
Mg^{2+}	wild-type	0.13 ± 0.01	38.40	1.02
	W573F	0.15 ± 0.01	32.57	1.13

binding three classes of herbicides. As AHAS requires three cofactors for the catalytic reaction, and little is known about the conserved W573 in the mobile loop, we have investigated the effect of W573 on the catalytic nature of the enzyme in detail.

The concentration of a half of the maximum velocity (K_m) for W573F increased approximately 22-fold over that of wild-type, suggesting that the mutation is near the substrate

binding site or its effect is transmitted to the site through a conformational change in the enzyme. Although the value of k_{cat} for the W573F is somewhat different (3-fold) from that of wild-type, agreeing with the results of Chong *et al.*,[8] the change is not of such a magnitude. However, the catalytic efficiency (k_{cat}/K_m) of W573F decreased to such a magnitude (2.47 to 0.036), indicating that this residue is involved in catalytic activity.

The $S_{0.5}$ of cofactors for wild-type AHAS decreased in the following order: ThDP ≈ Mg^{2+} > FAD. However, the $S_{0.5}$ for W573F AHAS decreased Mg^{2+} > ThDP > FAD. The $S_{0.5}$ for Mg^{2+} and FAD for the W573F increased 4-fold (0.56 and 1.29 to 2.18 and 4.93, respectively) over that of wild-type. However, the $S_{0.5}$ for ThDP for W573F decreased 3-fold (0.78 to 0.23) from that of the wild-type enzyme. These results suggest that a substitution at W573 caused significant perturbations in the activation process in the binding site of ThDP (*vide infra*).

ThDP is located centrally in the active site spanning the two monomers. The diphosphate portion of ThDP interacts with Mg^{2+} and with amino acid residues from the γ-domain. As in all other ThDP-dependent enzymes, the role of the

554 *Bull. Korean Chem. Soc.* **2006**, Vol. 27, No. 4

Masud Karim et al.

metal ion is the same; it acts as an anchor to hold the ThDP in place by coordinating with two of the phosphate oxygen atoms and two amino acid side chains.[2] The mobile loop region of tobacco (567-582), corresponding region of yeast (580-595), is near the active site. This region in yeast contains residues that are known to be important in substrate specificity (Trp586) and herbicide resistance (Met582, Val583, Trp586 and Phe590).[6] Although the mobile loop is not folded into any distinct secondary structure and is not within contact distance of the cofactors, this loop region closes over the active site and forms direct interactions with reaction intermediates as well as herbicidal inhibitors during catalysis. The magnitude reduction of the catalytic efficiency of W573F is attributed to the decline of the interaction between mobile loop regions near the side chain of W573 and the reaction intermediates.

We have shown previously that the substrate saturation curve did not follow Michaelis-Menten kinetics,[17] a general feature of plant AHASs was observed.[18,19] Using a discontinuous assay, the cofactor saturation curves showed negatively cooperative kinetics.[20] It has also been reported that for barley,[21] *Arabidopsis thaliana*[22] and *Serratia marcescens*[23] AHAS, reactivation by cofactors was time-dependent. We have also observed lags of a few minutes before attainment of full activity after addition of the cofactor. The W573F mutant exhibited a distinct lag phase in product formation when assayed without prior incubation with cofactors (data not shown). The Hill coefficient (n) for the W573F (0.86) was similar to that of the wild-type (0.75), suggesting that tryptophan at position 573 is very important in activity and cooperativity.

The quenching of tryptophan fluorescence provides a direct tool for the determination of the dissociation constant of a protein-ligand complex. However, the sensitivity of the method depends on the number and location of the fluorophores. Tobacco AHAS exhibited intrinsic fluorescence characteristics by the presence of tryptophan residues, very likely buried in the protein as revealed by a low fluorescence emission maximum (340-345 nm) upon excitation at 300 nm.[9]

The K_d of pyruvate, Mg^{2+} and ThDP for wild-type and W573F AHAS exhibited similar behavior when titrated in the presence and absence of the other cofactors. The tryptophan at position 573 is located on the termini of the mobile loop in the C-terminal region of AHAS near the active site, and is repositioned during catalysis as the mobile loop is confined by packing forces when ThDP and Mg^{2+} are combined in the active site.[6] In the previous result of yeast AHAS structure,[5,6] mobile loop and C-terminal region which involved in the formation of a substrate access channel were very labile, but in the presence of the CE, AHAS inhibitor, became ordered. Accordingly, these results imply that the substrate or cofactors binding itself into the deep channel of the active site was not affected by a single mutant (W573F) of the mobile loop in the C-terminal region. However, the substitution caused significant perturbations in the binding site during the enzyme reaction (*vide ante*). It can be anticipated that W573 binds with pyruvate through the interaction of hydrogen bonding, so that substrate affinity for W573 was highly decreased. Then, over all the reaction catalysis is delayed. These variations of active site might not be affected to the enzyme stability from the thermostability study which showed a little difference (~4 °C) of transition temperature between wild-type and W573F mutant.

The K_d of FAD for the W573F increased approximately two times more than that of the wild-type in the presence and absence of the other cofactors. FAD is bound in an extended conformation and is located in a crevice bounded by all three domains.[6] The high affinity (μM range rather than mM range of K_d) of FAD is due to numerous hydrogen bonds and van der Waals interactions between FAD and the enzyme based on crystallographic analysis. The FAD molecule does not appear to play a direct role in stabilization of the dimer interface since there is the only one hydrophobic contact (C8 methyl group of the flavin ring and Phe201' from the second monomer in yeast) to the second monomer.[6] However, they have proposed that FAD could participate directly in catalysis. Kim *et al.*[20] have suggested that FAD binding does not play any active role in catalysis due to no affinity difference whether the other cofactors (ThDP and Mg^{2+}) are present or not. It has been proposed that FAD is a vestigial remnant reflecting the evolution of AHAS from a POX-like ancestor.[6] Therefore, it appears that the position 573 at the mobile loop of the C-terminus is important to binding with FAD for structural reasons, maintaining the enzyme active site in the required geometry for catalysis to occur.

Strong interest has been raised in AHAS since several structurally unrelated classes of herbicides, including the sulfonylureas, the imidazolinones, the triazolopyrimidines, and the pyrimidyl-oxybenzoates, have been shown to specifically inhibit the enzyme.[24-27] The mutant studies have shown that several sites (G62, A63, V137, A146, K197, M292, D316 and V513 etc.) can lead to herbicide resistance. The one of most frequent mutation is W573 which has been found in *E. coli*, yeast, oilseedrape, tobacco, and cocklebur.[28-31]

References

1. Umbarger, H. E. *Annu. Rev. Biochem.* **1978**, *47*, 532-606.
2. Duggleby, R. G.; Pang, S. S. *J. Biochem. Mol. Biol.* **2000**, *33*, 1-36.
3. Chang, Y. Y.; Wang, A. Y.; Cronan, Jr. J. E. *J. Biol. Chem.* **1993**, *268*, 3911-3919.
4. Macheroux, P.; Schmid, J.; Amrhein, N.; Schaller, A. *Planta* **1999**, *207*, 325-334.
5. Pang, S. S.; Guddat, L. W.; Duggleby, R. G. *Acta Crystallogr. D Biol. Crystallogr.* **2001**, *57*, 1321-1323.
6. Pang, S. S.; Duggleby, R. G.; Guddat, L. W. *J. Mol. Biol.* **2002**, *317*, 249-262.
7. Yoon, M. Y.; Hwang, J. H.; Choi, M. K.; Baek, D. K.; Kim, J.; Kim, Y. T.; Choi, J. D. *FEBS Lett.* **2003**, *555*, 185-191.

8. Chong, C. K.; Shin, H. J.; Chang, S. I.; Choi, J. D. *Biochem. Biophys. Res. Commun.* **1999**, *259*, 136-140.

9. Kim, J.; Baek, D. G.; Kim, Y. T.; Choi, J. D.; Yoon, M. Y. *Biochem. J.* **2004**, *384*, 59-68.

10. Chang, S. T.; Kang, M. K.; Choi, J. D.; Namgoong, S. K. *Biochem. Biophys. Res. Commun.* **1997**, *234*, 549-553.

11. Oh, K. J.; Park, E. J.; Yoon, M. Y.; Han, J. R.; Choi, J. D. *Biochem. Biophys. Res. Commun.* **2001**, *282*, 1237-1243.

12. Yoon, T. Y.; Chung, S. M.; Chang, S. I.; Yoon, M. Y.; Hahn, T. R.; Choi, J. D. *Biochem. Biophys. Res. Commun.* **2002**, *293*, 433-439.

13. Westerfeld, W. W. *J. Biol. Chem.* **1943**, *161*, 495-502.

14. Lee, Y. T.; Chang, A. K.; Duggleby, R. G. *FEBS Lett.* **1999**, *452*, 341-345.

15. Dawson, R. M. C.; Elliott, D. C.; Elliott, N. H.; Johnes, K. M. *Data for Biochemical Research*, 2nd ed.; Oxford University: 1979; p 423.

16. Cleland, W. W. *Methods Enzymol.* **1979**, *63*, 103-138.

17. Hwang, J.; Kim, J.; Kim, Y. T.; Choi, J. D.; Yoon, M. Y. *Bull. Korean Chem. Soc.* **2003**, *24*, 1856-1858.

18. Schloss, J. V.; Van Dyk, D. E.; Vasta, J. F.; Kutny, R. M. *Biochemistry* **1985**, *24*, 4952-4959.

19. Chang, A. K.; Duggleby, R. G. *Biochem. J.* **1998**, *333*, 765-777.

20. Kim, J.; Kim, J. R.; Kim, Y. T.; Choi, J. D.; Yoon, M. Y. *Bull. Korean Chem. Soc.* **2004**, *25*, 721-725.

21. Miflin, B. J. *Arch. Biochem. Biophys.* **1971**, *146*, 542-550.

22. Chang, A. K.; Duggleby, R. G. *Biochem. J.* **1997**, *327*, 161-169.

23. Yang, J. H.; Kim, S. S. *Biochim. Biophys. Acta* **1993**, *1157*, 178-184.

24. Ibadah, M.; Bar-Ilan, A.; Livnah, O.; Schloss, J. V.; Barak, Z.; Chipman, D. M. *Biochemistry* **1996**, *35*, 16282-16291.

25. LaRossa, R. A.; Schloss, J. V. *J. Biol. Chem.* **1984**, *259*, 8753-8757.

26. Shaner, D. L.; Anderson, P. C.; Stidham, M. A. *Plant Physiol.* **1984**, *76*, 545-546.

27. Hattori, J.; Brown, D.; Mourad, G.; Labbe, H.; Ouellet, T.; Sunohara, G.; Rutledge, R.; King, J.; Miki, B. *Mol. Gen. Genet.* **1995**, *246*, 419-425.

28. Falco, S. C.; McDevitt, R. E.; Chui, C. F.; Hartnett, M. E.; Knowlton, S.; Mauvais, C. J.; Smith, J. K.; Mazur, B. J. *Dev. Ind. Microbiol.* **1989**, *30*, 197-194.

29. Hattori, J.; Brown, D.; Mourad, G.; Labbe, H.; Ouellet, T.; Sunohara, G.; Rutledge, R.; King, J.; Miki, B. *Molec. Gen. Genet.* **1995**, *246*, 419-425.

30. Lee, K. Y.; Townsend, J.; Tepperman, J.; Black, M.; Chui, C. F.; Mazur, B.; Dunsmuir, P.; Bedbrook, J. *EMBO J.* **1988**, *7*, 1241-1248.

31. Bernasconi, P.; Woodworth, A. R.; Rosen, B. A.; Subramanian, M. V.; Siehl, D. L. *J. Biol. Chem.* **1995**, *270*, 17381-17385.